Study of effects of confinement on vortex structure in dilute Bose-Einstein condensate

A Thesis

submitted to
Indian Institute of Science Education and Research Pune
in partial fulfillment of the requirements for the
BS-MS Dual Degree Programme

by

Arushi Bodas
Reg. No: 20121107
Supervised by: Prof. Arijit Bhattacharyay

Indian Institute of Science Education and Research Pune
Dr. Homi Bhabha Road,

Pashan, Pune 411008, INDIA.

April, 2017

Supervisor: Prof. Arijit Bhattacharyay

© Arushi Bodas 2017

All rights reserved

Certificate

This is to certify that this dissertation entitled ‘Study of effects of confinement on vortex structure in dilute Bose-Einstein condensate’ towards the partial fulfilment of the BS-MS dual degree programme at the Indian Institute of Science Education and Research, Pune represents study/work carried out by Arushi Bodas at Indian Institute of Science Education and Research under the supervision of Prof. Arijit Bhattacharyay, Department of Physics , during the academic year 2016-2017.

Arijit Bhattacharyay

Prof. Arijit Bhattacharyay

29.04.2017.

Arushi

Arushi Bodas

Committee:

Prof. Arijit Bhattacharyay

Prof. Rejish Nath

This thesis is dedicated to my mother, Neha Bodas
who gives me strength to pursue my dreams..

Declaration

I hereby declare that the matter embodied in the report entitled 'Study of effects of confinement on vortex structure in dilute Bose-Einstein condensate' are the results of the work carried out by me at the Department of Physics, Indian Institute of Science Education and Research Pune, under the supervision of Prof. Arijit Bhattacharyay and the same has not been submitted elsewhere for any other degree.

Arushi

Arushi Bodas

Acknowledgments

I would like to thank my supervisor Prof. Arijit Bhattacharyay for being such a supportive and patient guide. His thoughtful insights have always given me a new perspective on the problem at hand. I thank my TAC, Prof. Rejish Nath for giving valuable suggestions. I would also like to thank my group members Abhijit, Supratik and Projjwal for many interesting discussions during group meetings. Special thanks to Abhijit, who has been a great friend and teacher to me.

Of course, this would have been impossible without the constant support of my family and friends. Thank you, Aai and Aditi, for being there when things didn't work out! Thank you Divya, Jerrin and Mithila for pushing me through tough times. Thank you, physics-room people, for being a constant source of entertainment and making this experience memorable!

I would also like to thank IISER-Pune and DST, India for providing financial support and necessary resources for the work done during this thesis.

Abstract

In this thesis, I study the effect of confinement on the core structure of vortex state in dilute Bose gases. Densely packed vortex lattice presents a possibility of observing many exotic phenomena like quantum melting and atomic quantum Hall states. One way to achieve such dense packing is to decrease vortex core width to allow accommodation of more vortices before the quantum melting transition. Confinement might play a key role in modulating vortex width below the conventional healing length limit. I have studied two different systems: 1) hard boundary confinement in the transverse direction with a fixed far field density, and 2) a weakly interacting gas in an axisymmetric harmonic trap and fixed number of particles. In the first case, calculations have been carried out in a mean field approach. I observe that the vortex width near the centre of the trap scales as the confinement length when it is of the order of healing length. But this approach breaks down near the edges and requires further analysis. In the second system, both the length scales of confinement play a role in determining the core width which can be further reduced by making the interactions attractive. The minimum achievable vortex width for a fixed trap depends on the strength of attractive interaction and the ratio of characteristic lengths in the transverse and radial direction.

Contents

Abstract **xi**

1 Introduction **1**

1.1 From a single vortex to vortex lattice 2

1.2 Condensate with ultra high rotation 3

1.3 Motivation 6

1.4 Relevant theoretical background 7

2 Hard confinement along z-direction **13**

2.1 Constant vortex width 14

2.2 Variation in vortex width along z 18

3 Axially-symmetric harmonic trap **25**

3.1 Variational approach 26

3.2 Changed ansatz: attractive BEC 30

4 Conclusion and future work **35**

Chapter 1

Introduction

The conceptual roots of Bose-Einstein condensate date back to 1925 when Einstein, based on the work by S.N Bose on the statistical description of photons, predicted a phase transition in a gas of non-interacting atoms. The phase transition was characterised by condensation of a macroscopic fraction of atoms in the lowest single particle state. It was in 1938 that London tried to describe the superfluidity in liquid helium as a manifestation of underlying condensed phase and the theory of Bose-Einstein condensate found practical application. It also formed the basis for the theory of superconductivity in terms of condensation of Cooper pairs. With the development of sophisticated ultra-cooling techniques, it was possible to reach low enough temperatures for the formation of Bose-Einstein condensate. In 1995, the first experimental signatures of Bose-Einstein condensate was observed in ultra-cold vapours of alkali atoms like ^{87}Rb, ^{23}Na and ^{7}Li ([1],[2],[3]).

These days, Bose-Einstein condensate can be formed relatively easily in ultracold dilute atomic vapours which allows for a more rigorous experimental verification of the theory. BEC exhibits many distinct and unusual features which makes its study interesting. The occurrence of quantised vortices is one such characteristic. The response of neutral condensate to a rotation, which is the formation of vortex states, is analogous to the response of charged particles in superconductors to a magnetic field. The possibility of quantised vortices in BEC was first predicted by Onsager(1949) and Feynman (1955) and was later verified experimentally by Hall and Vinen (1956). These topological objects are a macroscopic manifestation of underlying quantum effects. Many properties of a single vortex as

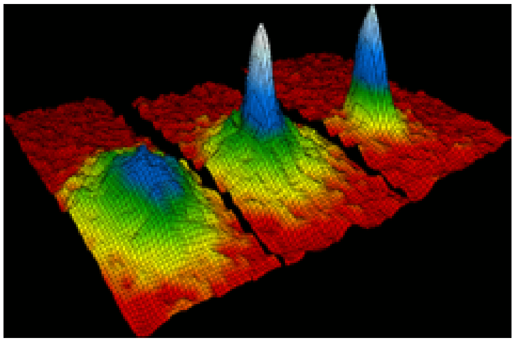

Figure 1.1: Image of velocity distribution of ^{87}Rb atoms as the temperature is lowered below a critical temperature for condensation from left to right. From [1]

well a vortex lattice up to about a hundred vortices have been well understood by mean field theory and rigorously studies experimentally. But it is generally in extreme limits that the system behaves most peculiarly, and our theory and experimental tools face real challenges. The following section will survey one such extreme limit of densely packed vortex lattice which serves as a motivation for the study conducted in this thesis.

1.1 From a single vortex to vortex lattice

Vortex states have higher energy than the ground state [4]. Thus an external torque is required to rotate the condensate. This can be achieved by introducing a slight anisotropy in the trap and then making it time dependent. The condensate then experiences a periodic time-dependent external potential. Just as a normal fluid kept in a rotating container starts rotating due to friction at the walls, the periodic V_{ext} imparts angular momentum to the condensate. After a certain frequency of rotation, the angular momentum is incorporated by the formation of a singly quantized vortex line.

In the presence of time-dependent potential $V_{ext}(\mathbf{r}, t)$, lab frame is no longer an appropriate frame of reference. It is necessary to shift to a frame rotating at the same frequency $\mathbf{\Omega}$ as the potential to see the stability of vortex. Let $H_{lab}(\mathbf{r}, \mathbf{p})$ be the Hamiltonian in the lab frame where $\mathbf{r}$ and $\mathbf{p}$ are the coordinates and conjugate momenta respectively and $\mathbf{L} = \mathbf{r} \times \mathbf{p}$ is the angular momentum. Then the Hamiltonian in a rotating frame $H_{rot}(\mathbf{r}', \mathbf{p}')$ is [4]

$$H_{rot}(\mathbf{r}', \mathbf{p}') = H_{lab}(\mathbf{r}', \mathbf{p}') - \mathbf{\Omega} \cdot \mathbf{L}(\mathbf{r}', \mathbf{p}')$$

where $\mathbf{r}'$ and $\mathbf{p}'$ are the coordinates and conjugate momenta in the rotating frame. The modified energy functional in the rotating frame is

$$E_{rot}[\Psi] = \int d\mathbf{r}' \left[\frac{\hbar^2}{2m}|\nabla\Psi(\mathbf{r}')|^2 + V_{ext}(\mathbf{r}')|\Psi(\mathbf{r}')|^2 + \frac{g}{2}|\Psi(\mathbf{r}')|^4\right] - \boldsymbol{\Omega}\cdot\int d\mathbf{r}'\ \Psi^*(\mathbf{r}')\ \boldsymbol{r}'\times\boldsymbol{p}'\ \Psi(\mathbf{r}')$$

The minimisation of energy now involves rotation frequency $\boldsymbol{\Omega}$ and the last term in above expression shows that non-zero angular momentum will be favoured.

As the rotation frequency is increased further, the extra angular momentum can be either stored by increasing angular momentum of a single vortex to higher quanta of circulation or by incorporating multiple singly quantized vortices. Vortex with multiple quanta of rotation is unstable and quickly breaks into many singly quantized vortices [5]. Thus, as the rotation is increased, the condensate expands and incorporates multiple vortex lines to form a lattice. These vortex lines are aligned parallel to the axis of rotation. The structure of this lattice has been studied in TF [6] as well as weak interaction limit [7]. See fig.(1.2)(A). The lattice has different symmetries depending on the number of vortex lines in the cloud. At large filling of vortices, they arrange into a hexagonal lattice (see fig.(1.2)(B)). The entire lattice rotates around the central axis and as the filling of vortex lines increases, the whole system tends to behave like a rigid rotator.

1.2 Condensate with ultra high rotation

At high rotational frequency, the number density of vortices in a 2D system changes as $n_v = \dfrac{m\Omega}{\pi\hbar}$ [4]). This equation shows that as the rotation frequency is increased, more and more vortex lines are packed together, and the vortices come closer to each other. When the inter-vortex distance becomes comparable to vortex width, they start to repel each other due to the centrifugal force of rotation. This further reduces the core size ([10],[11]). Eventually, inter-vortex spacing becomes of the order of core width. As Ω approaches the trap frequency ω, the ratio of the area per vortex and core area becomes constant ([10],[11],[12]), and the rotating condensate enters mean-field quantum Hall limit. In this limit, the centrifugal force balances the trapping potential in r-direction and the condensate expands considerably. This expansion leads to a substantial drop in the density. Since interaction energy scales as n^2, the decrease in density makes interaction energy much smaller than the energy scale of the trap

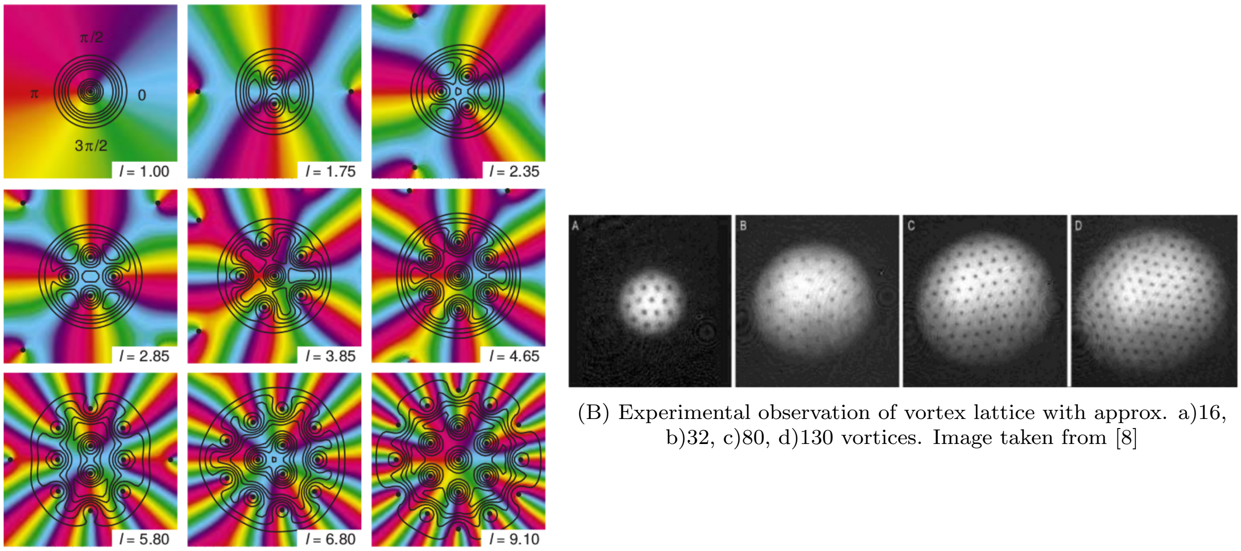

(A) Numerical simulation of vortex lattice in weak interaction regime. Black dots are the positions of vortices. l is the angular momentum per particle. Taken from [7]

(B) Experimental observation of vortex lattice with approx. a)16, b)32, c)80, d)130 vortices. Image taken from [8]

Figure 1.2: Structure of vortex lattice: numerical simulation and experimental observation.

$(\hbar\omega)$. The energy of the condensate then becomes equivalent to the energy of an electron in an effective magnetic field $\mathbf{B} = -2m\omega/|e|$ in the symmetric gauge whose spectrum is given by Landau levels. Essentially, ultra fast rotation in cold neutral atoms creates a similar effect as strong magnetic field in an electron system. Following this analogy, it was predicted that atoms in a rapidly rotating cloud of Bose gas should condense in the lowest Landau level (LLL) [13]. The many-body wavefunction in the mean field regime is given as

$$\Psi(z_1, z_2, ...) = \prod_i^N \prod_j (z_i - \eta_j) e^{-\frac{|z_i|^2}{2d_r^2}} \tag{1.1}$$

where $z = x + iy$, $d_r = \sqrt{\hbar/m\omega}$ is the characteristic length of the trap in r-direction and η_j are the positions of the vortex lines. The mean field quantum hall limit has been reached experimentally at $\Omega = 0.99\omega$ for about 500 atoms per vortex i.e filling fraction $\nu \sim 500$ [14].

Many interesting phenomena have been predicted when the frequency of rotation approaches trap frequency. At very high rotation, quantum fluctuations in the coordinates of the vortex become significant. As more and more vortices are pumped in the cloud, they are compressed together to the point that these quantum fluctuations become comparable

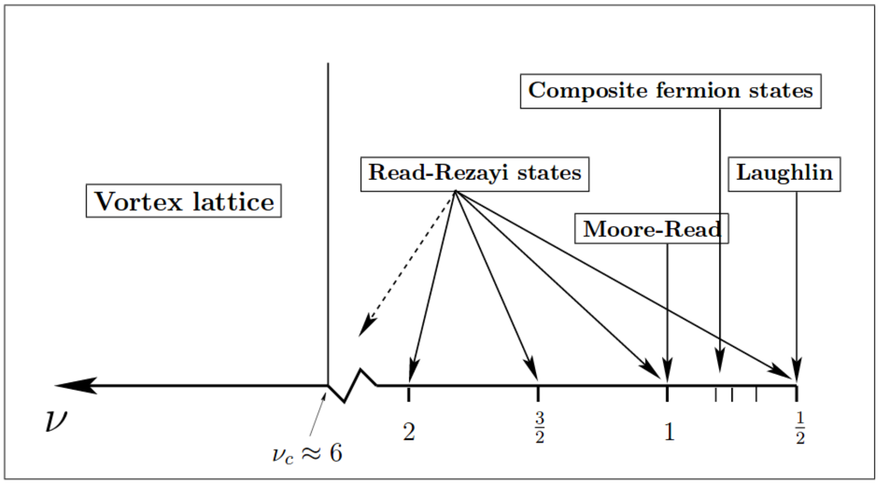

Figure 1.3: Theoretical characterization of different atomic quantum Hall states in rapidly rotating dilute Bose gas. Figure taken from [9]

to inter-vortex separation. At this point, vortices lose a fixed position, and the lattice breaks down. This phenomenon is termed as the quantum melting transition [15]. The angular momentum in this state is carried uniformly by a 'vortex fluid'.

A small filling fraction ν (average number of atoms per vortex) is required for the Lindemann criterion (average fluctuation in the position equals inter-vortex separation) to be satisfied [16]. Through analytical and numerical studies, the critical filling fraction ν predicted for such melting transition is $\nu_c \approx 8 - 10$. In this regime of ultra-fast rotation, The vortex fluid has been proposed to show many quantum liquid states ([16],[17],[18]). Extending the previous analogy of an electron in a strong transverse magnetic field, these quantum liquid states can be characterised as bosonic fractional quantum Hall states. Fig.(1.3) shows different atomic quantum Hall states at various filling fractions. Some of these states show special features. Properties of quasi-particle excitations of Read-Rezayi [19] states can be described by non-Abelian statistics. The 'composite fermion states' is another important class [20]. Analogous to the concept of a composite particle of an electron coupled to a unit magnetic flux, these composite states may occur from the coupling of a boson to a vortex carrying unit vorticity and thus experience reduced vorticity compared to the original system. It is clear that there is very rich physics at low filling fractions of vortex lattice and this regime is yet to be fully explored experimentally.

1.3 Motivation

As mentioned before, there have been experimental attempts to reach small filling fractions required for the manifestation of these quantum Hall states. Schweikhard *et al.* successfully reached $\nu \sim 500$ at $\Omega = 0.99\omega$ [14]. But this is still two orders of magnitude greater than required. The technical difficulty is that as Ω approaches ω, the trap becomes more and more unstable and at $\Omega = \omega$, it breaks down. There was an attempt to bypass this problem by considering a quartic potential $\frac{1}{4}kr^4$ so that Ω can be pushed beyond ω [21]. But the observations of this experiment are not conclusive. Recently, a new approach has developed where the vortices can be formed in an optical lattice without any rotation of the trap ([22],[23]). This opens up a new way of reaching atomic quantum Hall regime by circumventing the technical difficulties involved in ultra-fast rotation.

Another way of reducing the filling fraction ν would be to increase the number of vortices, N_v, while keeping the number of atoms, N, constant. This is possible if more vortices could be pumped in at the same rotation speed Ω. If the core width of a vortex could be modulated by some other experimental parameter apart from rotation speed, it could be used to further reduce vortex width at the same Ω which will allow accommodation of more vortices. A 10 fold decrease in the vortex width will increase the vortex density by a factor of 100, which will be sufficient to reach atomic quantum Hall regime.

Conventionally, healing length is defined as the length scale at which any perturbation in the condensate smoothens out to a uniform density. Thus, the width of vortex core is taken to be of the order of healing length (ξ), at least in a large system where boundary conditions do not affect the vortex structure [24]. The theme of this thesis is to devise ways to change the healing length dependence of vortex width to some other experimental parameter. Most of the focus would be on studying dilute Bose gas in different confinement geometries. Confinement provides an extra length scale apart from the microscopic length scale present in the system *i.e.* healing length. The hope is that this competing length scale might show some effect on the vortex width in certain regimes which can later be exploited to reduce the filling fraction in the vortex lattice.

We will assume the validity of mean field theory for the systems and parameter regions considered in this study. The theoretical background necessary to understand the analysis in this thesis is described in the following section. In chapter 2, a system confined in z-direction by hard boundaries while infinite in r-extent is studied. In chapter 3, we will introduce confinement in r as well. A system with axially-symmetric harmonic trap is studied in weak interaction regime. Conclusion and future work is presented in the end.

1.4 Relevant theoretical background

1.4.1 Mean field approach: Gross-Pitaevskii equation

The details of the theory presented in this section can be found in ([24],[5]). Bose-Einstein condensate is characterised by a macroscopic occupation of a single-particle state. This allows the use of Bogoliubov approximation such that the field operator can be split as a classical field and a fluctuation operator [24]

$$\hat{\mathbf{\Psi}}(\mathbf{r}) = \Psi_0(\mathbf{r}) + \delta\hat{\mathbf{\Psi}}(\mathbf{r}) \tag{1.2}$$

Bogoliubov approximation essentially ignores the non-commutativity of the field operator $\hat{a}_0$ since $< \hat{a}_0^\dagger \hat{a}_0 >= N >> 1$. In such case, $\varphi_0 \hat{a}_0 \approx \sqrt{N}\varphi_0 = \Psi_0$ where φ_0 is the single-particle wave function which is macroscopically occupied. $\delta\hat{\mathbf{\Psi}}(\mathbf{r})$ is the fluctuation on top of condensate. At low density and low temperatures required to attain BEC phase transition, this fluctuation term can be neglected and $\hat{\mathbf{\Psi}}(\mathbf{r}) \approx \Psi_0(\mathbf{r})$. This classical field $\Psi_0(\mathbf{r})$ is the order parameter of phase transition and $|\Psi_0(\mathbf{r})|^2$ gives the density of condensate n.

Dynamical equation for $\Psi_0(\mathbf{r})$: Hamiltonian of the system in terms of the field operator can be given as

$$\hat{H} = \int \left(\frac{\hbar^2}{2m} \nabla \hat{\mathbf{\Psi}}^\dagger \nabla \hat{\mathbf{\Psi}} + V_{ext} \hat{\mathbf{\Psi}}^\dagger \hat{\mathbf{\Psi}} \right) d\mathbf{r} + \frac{1}{2} \int \hat{\mathbf{\Psi}}^\dagger \hat{\mathbf{\Psi}}^{\dagger\prime} V(\mathbf{r}' - \mathbf{r}) \hat{\mathbf{\Psi}} \hat{\mathbf{\Psi}}' d\mathbf{r}' d\mathbf{r} \tag{1.3}$$

In the Heisenberg picture, the dynamical equation can be derived from

$$\begin{aligned} i\hbar \frac{\partial \hat{\mathbf{\Psi}}(\mathbf{r},t)}{\partial t} &= \left[\hat{\mathbf{\Psi}}(\mathbf{r},t), \hat{H} \right] && (1.4) \\ &= \left[-\frac{\hbar^2}{2m} \nabla^2 + V_{ext}(\mathbf{r},t) + \int \hat{\mathbf{\Psi}}^\dagger(\mathbf{r}',t) V(\mathbf{r}' - \mathbf{r}) \hat{\mathbf{\Psi}}(\mathbf{r}',t) d\mathbf{r}' \right] \hat{\mathbf{\Psi}}(\mathbf{r},t) && (1.5) \end{aligned}$$

At low density, only two body interactions are dominant. Also, at low temperatures needed for BEC, Born approximation is valid, and it is sufficient to consider only s-wave scattering. This allows the use of effective soft potential V_{eff} such that it produces same low energy scattering properties given by real interaction potential V. Also, there is a condition on the density of condensate $a_s n^{1/3} << 1$ where a_s is the s-wave scattering length. This implies that the inter-particle distance $n^{1/3}$ is much larger than a_s. This justifies the assumption that the order parameter $\Psi_0(\mathbf{r}, t)$ varies slowly over distances of the order of the range of inter-atomic interaction potential. Putting all this together, the last term in Eq.(1.4) becomes

$$\int \Psi_0^*(\mathbf{r}+\mathbf{s}, t) V_{eff}(\mathbf{s}) \Psi_0(\mathbf{r}+\mathbf{s}, t) d\mathbf{s} \approx |\Psi_0(\mathbf{r}, t)|^2 \int V_{eff}(\mathbf{s}) d\mathbf{s} \tag{1.6}$$

Let us define $g = \int V_{eff}(\mathbf{s}) d\mathbf{s}$ where g signifies the strength of interaction and is related to scattering length as $g = \dfrac{4\pi\hbar^2 a_s}{m}$. Thus the dynamical equation for order parameter is

$$i\hbar \frac{\partial \Psi_0(\mathbf{r}, t)}{\partial t} = \left[-\frac{\hbar^2}{2m} \nabla^2 + V_{ext}(\mathbf{r}, t) + g|\Psi_0(\mathbf{r}, t)|^2 \right] \Psi_0(\mathbf{r}, t) \tag{1.7}$$

Above equation is called time-dependent Gross-Pitaevkii equation (GPE).

Using Eq.(1.2), $\Psi_0(\mathbf{r}) =< N|\hat{\mathbf{\Psi}}(\mathbf{r})|N+1 >$. Considering the time evolution of the stationary states be governed by energy of that state,

$$\begin{aligned} \Psi_0(\mathbf{r}, t) &= < N| e^{iE(N)t/\hbar} \hat{\mathbf{\Psi}} e^{-iE(N+1)t/\hbar} |N+1 > \\ &= \Psi_0(\mathbf{r}) e^{-i(E_{N+1} - E_N)t/\hbar} \\ &= \Psi_0(\mathbf{r}) e^{-i\mu t/\hbar} \end{aligned}$$

where μ is the the energy required to put one extra particle in the condensate, or in other words, μ is the chemical potential of the system. Unlike single particle states, the time evolution of order parameter Ψ_0 is governed by chemical potential rather than energy. Putting this in Eq.(1.7), we get stationary GPE

$$\left[-\frac{\hbar^2}{2m} \nabla^2 + V_{ext}(\mathbf{r}) + g|\Psi_0(\mathbf{r})|^2 \right] \Psi_0(\mathbf{r}) = \mu \Psi_0(\mathbf{r}) \tag{1.8}$$

The stationary GPE can also be obtained by minimising energy of the system under the constraint of fixed particle number, that is, $\delta(E - \mu N) = 0$ where μ acts as a Lagrange multiplier. This is same as minimising the variation of grand potential with respect to Ψ_0^*.

The wavefunction can also be written in terms of amplitude $\sqrt{n(\mathbf{r},t)}$ and phase $S(\mathbf{r},t)$ as

$$\Psi_0 = \sqrt{n(\mathbf{r},t)}e^{iS(\mathbf{r},t)}$$

Using this wavefunction, the current density can be given as

$$\boldsymbol{j}(\mathbf{r},t) = \frac{1}{2m}\left(\Psi_0^* \hat{\boldsymbol{p}}\Psi_0 + c.c.\right) = n\frac{\hbar}{m}\nabla S(\mathbf{r},t)$$

Comparing this with the expression of flow density in continuity equation, $\boldsymbol{j}(\mathbf{r},t) = \boldsymbol{n}\cdot\boldsymbol{v}$, we get the velocity field as

$$\boldsymbol{v}(\mathbf{r},t) = \frac{\hbar}{m}\nabla S(\mathbf{r},t)$$

Since velocity field can be written as a gradient of another field, $\nabla \times \boldsymbol{v} = 0$, *i.e.* the flow in BEC is irrotational.

1.4.2 Structure of vortex states

Many important features of vortices have been successfully explained by the mean field Gross-Pitaevskii equation which was described in the previous section. It will be used in this section to highlight some characteristic features of vortex states. Rotations in superfluids have very different properties than in normal systems which make their study interesting. In a normal fluid, the velocity field corresponds to that of a rigid rotator and has the form $\boldsymbol{v} = \Omega \times \mathbf{r}$ giving a vorticity curl $\nabla \times \boldsymbol{v} = 2\Omega \neq 0$. But as described in the previous section, BEC is an irrotational fluid (which is a characteristic of any superfluid) implying $\nabla \times \boldsymbol{v} = 0$. This property gives a very different velocity field than that of a rigid rotator.

In this section, we will review some of the properties of a straight vortex line in an otherwise uniform condensate of really large extent. Due to axial symmetry of the vortex state, we would work in cylindrical coordinates (r,θ,z). For a state corresponding to rotation about central axis in a large system, we can consider an ansatz $\Psi_0(\mathbf{r}) = |\Psi_0(r)|e^{is\theta}$. Due to the symmetry of the state, the norm $|\Psi_0|$ only depends on r. Notice,

$$\hat{l}_z\Psi_0 = -i\hbar\frac{\partial}{\partial\theta}\Psi_0 = s\hbar\Psi_0$$

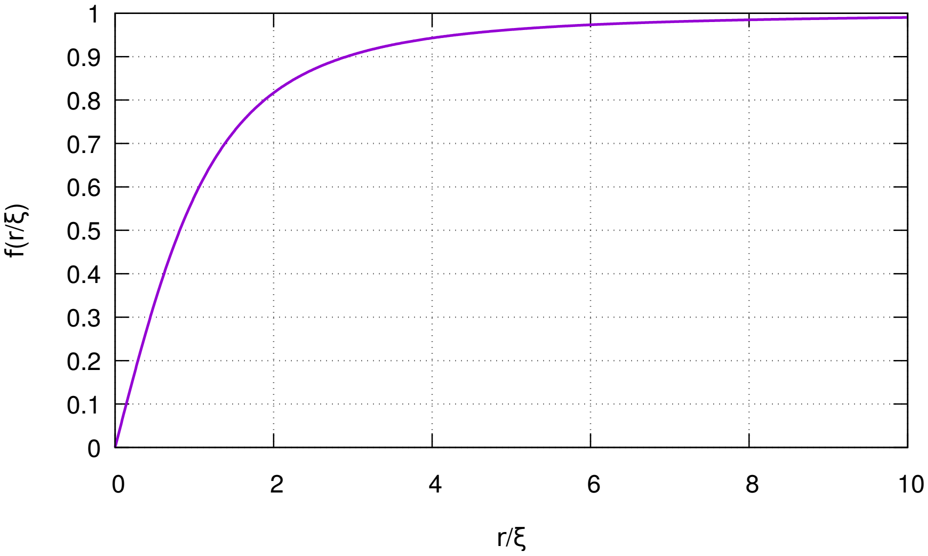

Figure 1.4: $f(\tilde{r}) = \dfrac{\tilde{r}}{\sqrt{\tilde{r}^2+2}}$ is plotted against $\tilde{r}$ where $\tilde{r} = r/\xi$ for $s = 1$

This means that the wavefunction is an eigenstate of the angular momentum operator with $l_z = s\hbar$. The total angular momentum of the vortex is equal to $L_z = Ns\hbar$. To ensure that the wavefunction $\Psi_0(\mathbf{r})$ is single valued, s has to be an integer. Thus, the angular momentum of the vortex state is quantized.

The velocity field can be computed from the phase factor S as $\boldsymbol{v}(\mathbf{r},t) = \dfrac{\hbar}{m}\nabla S(\mathbf{r},t)$. Here, $S(\mathbf{r},t) = s\theta$ giving $\boldsymbol{v} = \dfrac{\hbar}{m}\dfrac{s}{r}\hat{\theta}$. The velocity decreases as r increases which is opposite of the rigid rotator case where velocity of rotation increases with r. Also the velocity shows divergence at $r = 0$. To avoid this, the wavefunction must have a node at $r = 0$ giving a void at the centre. Also, the circulation of velocity over a closed contour around z-axis can be evaluated to be

$$\oint \boldsymbol{v}.d\mathbf{l} = \int_\theta \frac{\hbar}{m}\frac{s}{r} r d\theta = 2\pi s \frac{\hbar}{m}$$

which is quantised in the units of $\hbar/m$ independent of the radius of the contour chosen.

To study the profile of order parameter $\Psi_0(r)$ for a vortex state, we have to go to the GPE in (r,θ) coordinates,

$$-\frac{\hbar^2}{2m}\left[\frac{1}{r}\partial_r(r\partial_r) - \frac{s^2}{r^2}\right]\Psi_0(r) + (V_{ext} - \mu)\Psi_0(r) + g|\Psi_0(r)|^2\Psi_0(r) = 0 \tag{1.9}$$

Far away from the core, the density of the gas should reach a constant value. At large r, the kinetic term in the GPE can be neglected to get $|\Psi_0(r)|^2 = \dfrac{\mu}{g} = n$. In a uniform state, $\mu = gn_0$ where n_0 is the density in unperturbed state. It can be shown that in the presence of a vortex, the corrections to chemical potential μ are of the order of $an_0^{1/3}$ and thus negligible [24]. Thus $n \approx n_0$. Putting $\Psi_0 = \sqrt{n} f(\tilde{r})$ where $\tilde{r} = r/\xi$ and $\xi = \hbar/\sqrt{2mgn}$, the GPE in dimensionless form looks as follows

$$\frac{1}{\tilde{r}}\frac{\partial}{\partial \tilde{r}}\left(\tilde{r}\frac{\partial f(\tilde{r})}{\partial \tilde{r}}\right) + \left(1 - \frac{s^2}{\tilde{r}^2}\right) f(\tilde{r}) - f(\tilde{r})^3 = 0 \tag{1.10}$$

with boundary conditions that $f(\tilde{r} = 0) = 0$ and $f(\tilde{r} \to \infty) = 1$. To study the behaviour of $f(\tilde{r})$ near $\tilde{r} = 0$, put an ansatz $f(\tilde{r}) \sim \tilde{r}^p$ and balance the leading order term,

$$(p^2 - s^2)\tilde{r}^{p-2} + \tilde{r}^p - \tilde{r}^{3p} = 0$$

For $\tilde{r} << 1$, the leading order term is $\tilde{r}^{p-2}$. Setting the coefficient of this term to 0, we get $p = s$. Thus the behaviour of vortex with angular quantum number s near the center $\sim \tilde{r}^s$. This implies that the wavefunction for a vortex with single quantum of rotation falls linearly near the center.

There is no exact analytical solution to GPE for vortex state but there are different ansatz which capture the the qualitative behaviour of the condensate profile. One such ansatz for $s = 1$ comes from Padé approximation and closely matches the numerical simulations. It is given as

$$f(\tilde{r}) = \frac{\tilde{r}}{\sqrt{\tilde{r}^2 + 2}} \tag{1.11}$$

The above function is plotted in Fig.(1.4). Notice that the core size is $\sim \xi$. Thus in a large system where the boundaries do not affect the core structure of the vortex, the core width V_w is of the order of ξ.

Chapter 2

Hard confinement along *z*-direction

In the study of vortex states, the density profile along r is of most interest and the effect of z confinement is generally suppressed to reduce complications in the calculation. This can be done by taking a large spatial extent in z-direction such that the change of density profile along z can be neglected to a good approximation and the boundary conditions in z do not significantly affect vortex dynamics near $z = 0$. In such systems, unless there is tight confinement in r, there is only one microscopic length scale, the healing length ξ, which naturally determines the scale of vortex core width V_w [5]. But, if the system is confined in z in such a way that the length scale of this confinement is comparable to ξ, then there is a possibility that both these length scales are involved in fixing the vortex width. What will be the expression for V_w in such a system? In this chapter, we will try to answer this question by rigorously studying the effect of z-confinement on the vortex profile. The effect of r confinement is studied in the next chapter.

We will consider a system with infinite r extent. This will allow us to analyse the effect of z-confinement solely. For simplicity, we will consider hard boundaries in z, *i.e*, an infinite potential well of length L, implying $\Psi(z = 0) = \Psi(z = L) = 0$. Basically, the system looks like a disc with a very large radius. The far field density in the middle of the trap is set to n. Fixing far field density also fixes healing length, ξ, as $\xi = 1/(8\pi a_s n)^{1/2}$. Since the extent in r is large, the change in L will not affect the far field density. This allows us to independently change L and ξ. We will be using a semi-variational approach as explained in the following section.

2.1 Constant vortex width

The grand potential energy of BEC system held at chemical potential μ is given by the expression

$$E_G[\Psi(\mathbf{r}), \Psi(\mathbf{r})^*] = \int d\mathbf{r} \left[\frac{\hbar^2}{2m} |\nabla \Psi(\mathbf{r})|^2 + V_{ext}(\mathbf{r}) |\Psi(\mathbf{r})|^2 + \frac{g}{2} |\Psi(\mathbf{r})|^4 - \mu |\Psi(\mathbf{r})|^2 \right] \tag{2.1}$$

$V_{ext}(\mathbf{r})$ is the extrenal trapping potential. The equation for a steady state can be obtained by minimising variation of E_G with respect to Ψ^*, $i.e$, by setting $\dfrac{\delta E_G}{\delta \Psi^*} = 0$, which gives the time independent Gross-Pitaevskii equation (GPE)

$$\left[-\frac{\hbar^2}{2m} \nabla^2 + V_{ext} + g |\Psi(\mathbf{r})|^2 \right] \Psi(\mathbf{r}) = \mu \Psi(\mathbf{r}) \tag{2.2}$$

The nonlinear term $g|\Psi(\mathbf{r})|^2$ comes from short ranged interactions in the mean field approach. This nonlinearity prevents separation of variables, making it difficult to obtain exact solution of GPE. Thus, we will adopt some suitable ansatz to simplify the calculation.

Let us take the wavefunction in the form $\Psi(r, \theta, z) = \sqrt{n} f(r) h(z) e^{i\theta}$. We will only consider vortex with unit angular momentum ($s = 1$). As explained in the introduction, numerical simulations in 2D systems have shown that the form of condensate profile in r-direction closely resembles the functional form $\dfrac{r}{\sqrt{r^2 + 2\xi^2}}$, where ξ acts as a scaling factor for r, or in other words, ξ is the length scale of vortex core width V_w. Similarly, we will consider an ansatz for $f(r)$ as,

$$f(r) = \frac{r}{\sqrt{r^2 + \beta^2}} \tag{2.3}$$

Notice that here β, which sets the length scale of V_w, is now a variational parameter. The aim is to find the dependence of β on L and ξ. To begin with, we take β as a constant parameter, but it can also have z dependence. The case of $\beta(z)$ is analysed in the next section. The calculation scheme is as follows:

1) Find the mean field equation for stationary state of *h(z)*: Putting the form of $f(r;\beta)$ as in (3.8) in the expression for E_G (2.1) and integrating over r, the grand energy is now only a functional of $h(z)$ and $h^*(z)$. Using the similar method as that used to obtain GPE (2.2), minimize E_G with respect to $h^*(z)$ to get the equation for $h(z)$. That is

$\dfrac{\delta E_G[h(z), h^*(z); \beta]}{\delta h^*(z)} = 0$ gives the equation for $h(z; \beta)$.

2) Obtain the form of *h(z)*: Solve the equation obtained from the previous step exactly to get $h(z)$. Notice that $h(z)$ will depend on the parameter β.

3) Minimize E_G with respect to β: Using $h(z)$, re-evaluate E_G, which will now depend only on the variational parameter β. As β varies, the grand potential of the system will also vary and at some particular value of β, E_G will be minimized. Thus, in the end, $\dfrac{\partial E_G(\beta)}{\partial \beta} = 0$ will give us the expression for β, and in effect, an expression for V_w.

2.1.1 Deriving equation for h(z)

The expression for E_G with given ansatz looks like

$$E_G = n \int_{r=0}^{R} \int_z 2\pi r dr dz \left[\frac{\hbar^2}{2m} \left\{ |\frac{\partial f}{\partial r}|^2 |h|^2 + \frac{|fh|^2}{r^2} + |f|^2 |\frac{\partial h}{\partial z}|^2 \right\} + \frac{gn}{2} |fh|^4 - \mu |fh|^2 \right] \tag{2.4}$$

$V_{ext} = 0$ since the potential inside the confinement is set to 0. Also, notice the upper limit on r integration (R) which has to be put by hand. This is because the energy of a single vortex is logarithmically diverging with respect to system size. To get any meaningful value for energy, we have to put an upper limit on the integral [5]. This upper limit R will be set to be large as compared to vortex width so that it does not affect the structure of vortex profile.

Evaluating $\dfrac{\delta E_G}{\delta h(z)^*} = 0$, we get

$$-\left(\int |f|^2\right) \frac{\partial^2 h(z)}{\partial z^2} + \left(\int |\frac{\partial f}{\partial r}|^2 + \frac{|f|^2}{r^2}\right) h(z) + \tilde{g} n \left(\int |f|^4\right) |h(z)|^2 h(z) - \tilde{\mu} \left(\int |f|^2\right) h(z) = 0 \tag{2.5}$$

$\tilde{g} = \dfrac{2m}{\hbar^2} g$ and $\tilde{\mu} = \dfrac{2m}{\hbar^2} \mu$. This is the equation for $h(z)$. For simplicity, we will write it in the form

$$\frac{\partial^2 h(z)}{\partial z^2} + C_2 h(z) - C_3 |h(z)|^2 h(z) = 0 \tag{2.6}$$

where

$$C_2 = \frac{\int -|\frac{\partial f}{\partial r}|^2 - \frac{|f|^2}{r^2} + \tilde{\mu}|f|^2}{\int |f|^2} = \frac{\left(\frac{-R^2(R^2+2\beta^2)}{2(R^2+\beta^2)^2} + Log\frac{\beta^2}{R^2+\beta^2}\right)}{\left(R^2 + \beta^2 Log\frac{\beta^2}{R^2+\beta^2}\right)} + \tilde{\mu}$$

and

$$C_3 = \frac{\int |f|^4}{\int |f|^2} = 2\tilde{g}n\frac{\left(\frac{R^2(R^2+2\beta^2)}{2(R^2+\beta^2)} + \beta^2 Log\frac{\beta^2}{R^2+\beta^2}\right)}{\left(R^2 + \beta^2 Log\frac{\beta^2}{R^2+\beta^2}\right)}$$

The β dependence in the coefficients C_2 and C_3 captures the effect of condensate profile in r-direction. The integration over r shows that we are considering an average effect of r dynamics on the equation of $h(z)$. This is in some sense a mean field approach. In the absence of vortex, $C_2 \to \tilde{\mu}$ and $C_3 \to \tilde{g}$. This shows that the presence of vortex renormalises the coefficients in the equation for $h(z)$.

The time evolution in BEC system is governed by chemical potential μ in mean field approach. Thus, consider $h(z) = \tilde{h}(z)e^{-i\mu t/\hbar}$. The vortex state typically has only tangential velocity, that is, the phase only has θ dependence. This implies $\tilde{h}(z)$ is now a real function. Let us change the variable z in Eq.(2.6) to a dimensionless variable $\tilde{z} = z/L$. Then the equation becomes

$$\frac{\partial^2 \tilde{h}}{\partial \tilde{z}^2} + C_2 L^2 \tilde{h} - C_3 L^2 \tilde{h}^3 = 0 \tag{2.7}$$

The general solution of Eq.(2.7) can be written in terms of Jacobi Elliptical functions [25]. The boundary conditions of the problem $\tilde{h}(\tilde{z} = 0) = \tilde{h}(\tilde{z} = 1) = 0$ prompt the use of Jacobi sn [1] function [26]. Consider the solution form as

$$\tilde{h}(\tilde{z}) = A\ sn(a\tilde{z} + \delta|m) \tag{2.8}$$

$\tilde{h}(z = 0) = 0$ implies $\delta = 0$. Also *sn* functions are periodic with a period of $4K(m)$ where $K(m)$ is the complete elliptical integral of first kind. The first node appears at half period *i.e.* at $2K(m)$. This along with the boundary condition $\tilde{h}(\tilde{z} = 1) = 0$ and Eq.(2.8) gives $a = 2jK(m)$ where $j \in \{1, 2, 3...\}$. The j^{th} solution has $j - 1$ nodes. Since we are interested in the ground state, we will choose the solution with minimum nodes i.e. $j = 1$. A is determined such that the far field density at $\tilde{z} = 1/2$ is n. At $\tilde{z} = 1/2$, $sn(K(m)|m) = 1$ $\forall m$. Thus $A = 1$. Putting $\tilde{h}(\tilde{z})$ in Eq.(2.7), we get

---

[1] The family of *sn* functions is parametrised by m, where $0 \le |m| \le 1$. When $m = 0$, $sn(x|0) = sin(x)$ and when $m = 1$, $sn(x|1) = tanh(x)$

$$\left[C_2L^2 - 4K(m)^2(1+m^2)\right] sn(2K(m)\tilde{z}|m) + \left[8K(m)^2m^2 - C_3L^2\right] sn^3(2K(m)\tilde{z}|m) = 0$$

For the equation to be satisfied at every $\tilde{z}$, the coefficients of both sn and sn^3 should be zero. This implies

$$C_2L^2 = 4K(m)^2(1+m^2) \tag{2.9}$$

and

$$C_3L^2 = 8K(m)^2m^2 \tag{2.10}$$

There are two unknowns, m and $\tilde{\mu}$, which will get determined from Eq(2.10) and Eq.(2.9) respectively, in terms of system parameters g and n, variational parameter (β) and the cutoff R.

2.1.2 Minimization of E_G with respect to β

Having obtained the entire form of Ψ, put it back in the expression(2.4) to evaluate E_G as a function of β.

$$E_G(\beta) = \frac{-gn^2}{2}2\pi\left(\frac{R^2(R^2+2\beta^2)}{2(R^2+\beta^2)} + \beta^2 Log\frac{\beta^2}{R^2+\beta^2}\right) L\left[\frac{-2(1+m^2)E(m)+(2+m^2)K(m)}{3m^4K(m)}\right] \tag{2.11}$$

$E(m)$ is the elliptical integral of second kind. Remember that here m itself depends on β.

As mentioned before, the vortex width V_w is of the order of ξ when $L, R >> \xi$. This behaviour should be reproducible with our analysis and thus can be used to check the validity of the employed mean field approach. For simplicity, we can write E_G as

$$E_G(\beta) = \frac{-\hbar^2 nL}{2m}2\pi\frac{R^2}{2\xi^2}E'(\beta)$$

where $E'(\beta)$ is a dimensionless quantity given as

$$E'(\beta) = \left(\frac{(R^2+2\beta^2)}{2(R^2+\beta^2)} + \frac{\beta^2}{R^2}Log\frac{\beta^2}{R^2+\beta^2}\right)\left[\frac{-2(1+m^2)E(m)+(2+m^2)K(m)}{3m^4K(m)}\right] \tag{2.12}$$

As can be seen from Eq.(2.11) and Eq(2.12), $E_G(\beta)$ and $E'(\beta)$ only differ by a multiplicative factor which is independent of β. Thus it is sufficient to plot $E'(\beta)$ as a function of β to understand the qualitative behaviour of grand potential E_G. m can be evaluated in terms of β from Eq.(2.10) and μ from Eq.(2.9).

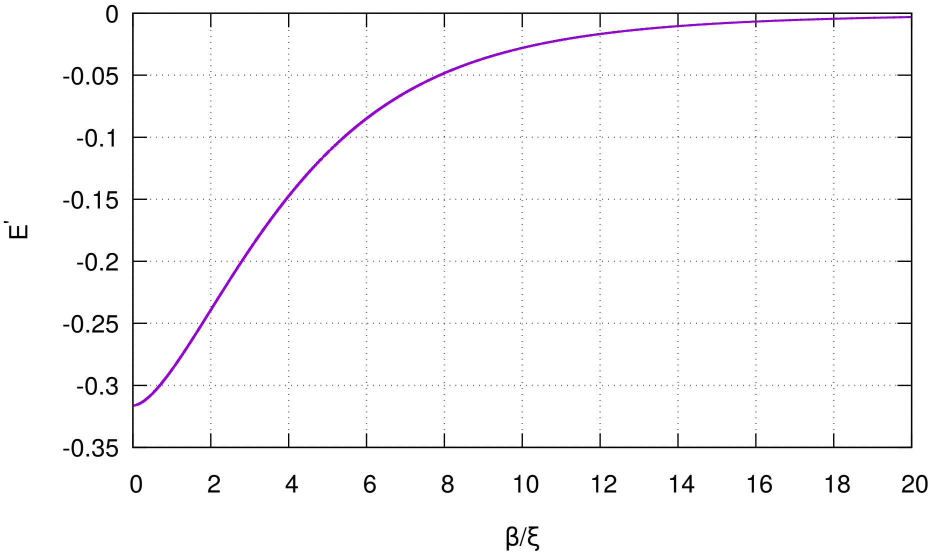

Figure 2.1: E' vs β/ξ curve for $L = 10\xi$ and $R = 10\xi$

Fig(2.1) shows $E'(\beta)$ as a function of β/ξ when $L = 10\xi$ and $R = 10\xi$. A minima was expected at $\beta/\xi \sim 1$. But it can be seen that energy is monotonically decreasing as $\beta \rightarrow 0$ and no minima is observed at $\beta/\xi \sim 1$. Since the current approach does not yield an expected answer in the large L limit, it is not entirely valid and requires improvements.

2.2 Variation in vortex width along z

Intuitively, the vortex width is expected to vary along z. Thus, the next step in improving the ansatz would be to consider β as a function of z. The ansatz then becomes

$$\Psi(r,\theta,z) = \sqrt{n} f(r,z) h(z) e^{i\theta} = \sqrt{n} \frac{r}{\sqrt{r^2+\beta^2(z)}} h(z) e^{i\theta} \tag{2.13}$$

Notice that β is no longer a parameter but a function and our previous calculation scheme needs to be changed accordingly.

New analysis scheme: E_G for new ansatz is a functional of a complex function $h(z)$ which captures the profile in z-direction and a real function $\beta(z)$ which accounts for the z dependence of vortex width. Thus we would get coupled equations for $h(z)$ and $\beta(z)$ by evaluating $\frac{\delta E_G}{\delta h^*(z)} = 0$ and $\frac{\delta E_G}{\delta \beta(z)} = 0$ simultaneously.

Similar approach has been used before to obtain quasi 1D and 2D GPE in the context of cigar shaped and disc shaped BEC respectively [27].

The potential energy will now have extra terms involving $\partial\beta(z)/\partial z$ which will show up in the kinetic energy term due to variation along z. This will be the only different term from E_G expression for previous calculations(2.4).

$$|\frac{\partial \Psi}{\partial z}|^2 = |h|^2 \left(\frac{\partial f}{\partial z}\right)^2 + f^2 |\frac{\partial h}{\partial z}|^2 + f \frac{\partial f}{\partial z}\frac{\partial |h|^2}{\partial z}$$

where $\frac{\partial f}{\partial z} = \frac{\partial f}{\partial \beta}\frac{\partial \beta(z)}{\partial z}$. Let us assume that $h(z)$ varies much faster along z than $\beta(z)$. Thus we can neglect terms involving $\partial\beta/\partial z$. This gives

$$E_G \approx n \int_{r=0}^{R} \int_z 2\pi r dr dz \left[\frac{\hbar^2}{2m}\left\{|\frac{\partial f}{\partial r}|^2 |h|^2 + \frac{|fh|^2}{r^2} + |f|^2 |\frac{\partial h}{\partial z}|^2\right\} + \frac{gn}{2}|fh|^4 - \mu |fh|^2\right]$$

which is the same as previous expression(2.4) except β is now a function of z.

Equation for $h(z)$, $\frac{\delta E_G}{\delta h^*(z)} = 0$ will be same as (2.6) with the same form of C_2 and C_3, only parameter β is replaced by a function $\beta(z)$. Equation for $\beta(z)$ is obtained by $\frac{\delta E_G}{\delta \beta(z)} = 0$

$$\begin{aligned} &-\beta\left\{Log\frac{\beta^2}{R^2+\beta^2} + \frac{R^2}{R^2+\beta^2}\right\}|\frac{\partial h}{\partial z}|^2 + \left\{\beta\left(Log\frac{\beta^2}{R^2+\beta^2} + \frac{R^2}{R^2+\beta^2}\right)\tilde{\mu}\right\}|h|^2 \\ &\left\{+\frac{R^2\beta^3}{(R^2+\beta^2)^3} + \frac{R^2}{\beta(R^2+\beta^2)}\right\}|h|^2 - \frac{\tilde{g}n}{2}\beta\left\{\frac{R^2(3R^2+2\beta^2)}{(R^2+\beta^2)^2} + 2Log\frac{\beta^2}{R^2+\beta^2}\right\}|h|^4 = 0 \end{aligned} \tag{2.14}$$

$\beta(z)$ depends on $\tilde{h}(z)$ as expected. The equations for $\beta(z)$ and $\tilde{h}(z)$ are nontrivially coupled which makes it very difficult to get the analytical form for these two functions. Thus, further analysis is done numerically.

As done previously, the relation $V_w \sim \xi$ needs to be checked when $L, R >> \xi$ to validate our approach. Let us first understand the behaviour of $\beta(z)$ near the center of the trap i.e. at $z = L/2$. In Eq.(2.14), $\tilde{h}(z = L/2) = sn(K(m)|m) = 1$ and $\left(\partial\tilde{h}/\partial z\right)_{z=L/2} = 0$. As before, m and μ are obtained from the equations for C_2(2.9) and C_3(2.10). With this approach, an energy minima exists. Its dependence on ξ in large L limit is shown in the following figure.

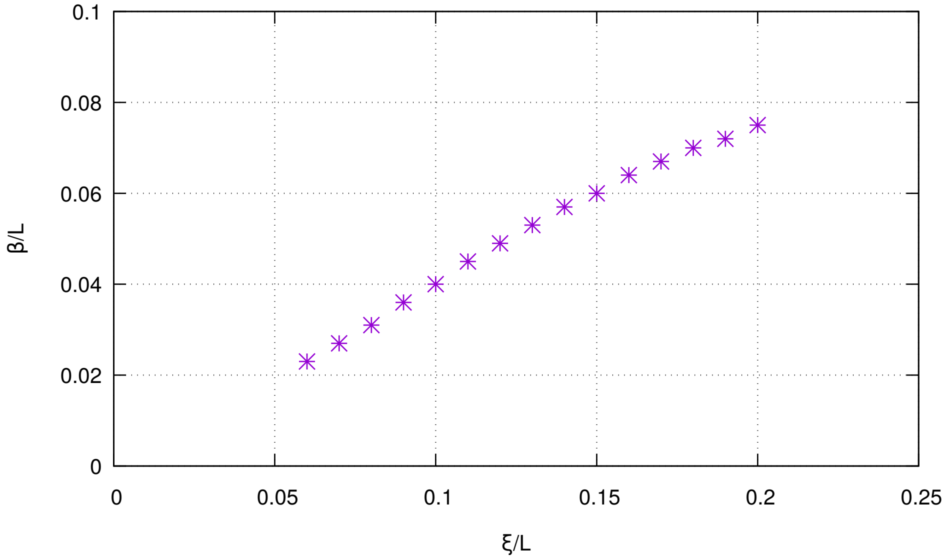

Figure 2.2: $\beta(z = L/2)/L$ vs ξ/L for fixed $L >> \xi$ ($L \sim R = 10\xi$)

Fig(2.2) shows that for a fixed L which is large as compared to ξ, $\beta(z = L/2)$ scales as ξ and thus vortex width $V_w \sim \xi$. Also note that the cutoff R is about 50-100 times the scale factor β. Thus an arbitrary cutoff in r is justified.

Having verified the approach, let us analyse the effect of variation of confinement length scale L on the vortex width at the center of the trap i.e $\beta(z = L/2)$. The healing length ξ will be fixed by fixing interaction strength g and far field density n. Also, R is set to be 10ξ. From the equation for C_3(2.10), it can be seen that modulation of confinement length L directly affects the parameter m of sn function. When L is small, m is closer to 0 and

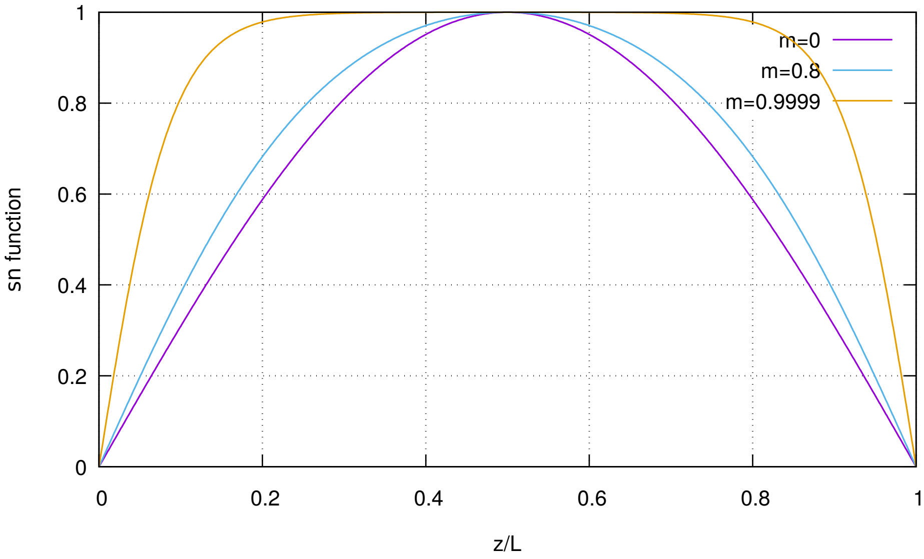

Figure 2.3: $sn(2K(m)\tilde{z}|m)$ vs $\tilde{z}$. The three curves correspond to different values of m. Purple: m=0 ; Blue: m=0.8 ; Yellow: m=0.9999.

the profile in z-direction is close to *sin* function (see Fig(2.3)). This is expected because as the confinement is made tighter, the kinetic energy dominates the interaction term and the wavefunction looks similar to the wavefunction for a particle in a box. In the other limit when L is very large, $m \to 1$ *i.e* $sn \to tanh$. This means that $\tilde{h}(z)$ would be almost constant in the middle of the trap (see Fig(2.3)) and the boundary conditions in z would not affect the vortex structure. This is consistent with our previous observation in Fig.(2.2) that $V_w \sim \xi$ when $L >> \xi$.

As L (and thus m) is changed, the chemical potential μ is also modulated through equation for C_2(2.9). Fig.(2.4) shows the L dependence of $\beta(z = L/2)$ when L is varied from $L \sim 0.1\xi$ to $L \sim 15\xi$ when $R = 10\xi$. There are two interesting features of this plot:

1) The plateau at large *L*: As explained before, when $L >> \xi$, we do not expect the vortex width in the middle of the trap to depend on L. The plateau-like behaviour of the curve is consistence with the expectation. In this region, $\beta \sim \xi$.

2) Linear increase for small *L*: when $L \sim \xi$, β is almost linearly dependent on L. That means for the confinement of the order of healing length, the vortex width (at least at the middle of the trap) can be modulated simply by modulating the confinement length.

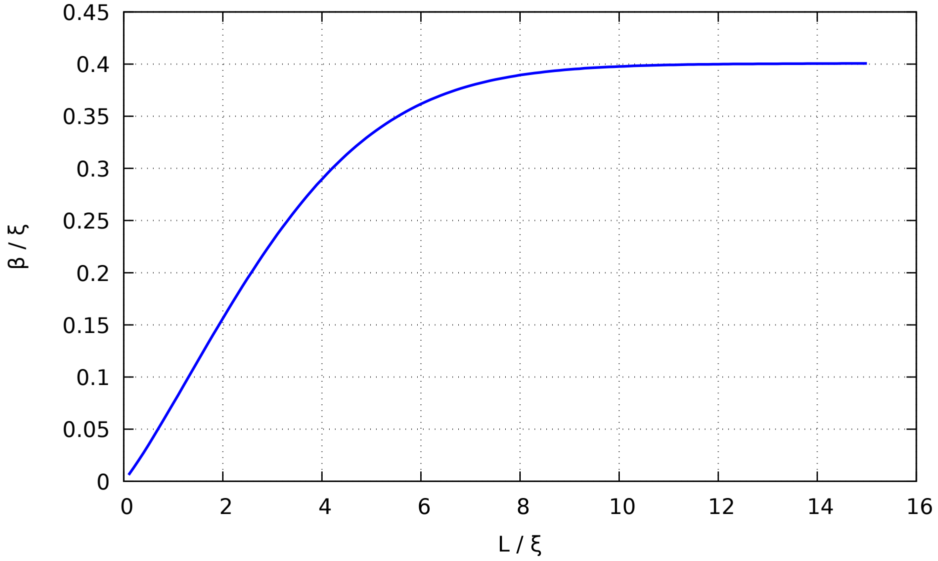

Figure 2.4: scaled β-vs-L at the centre of the trap *i.e.* at $z = L/2$.

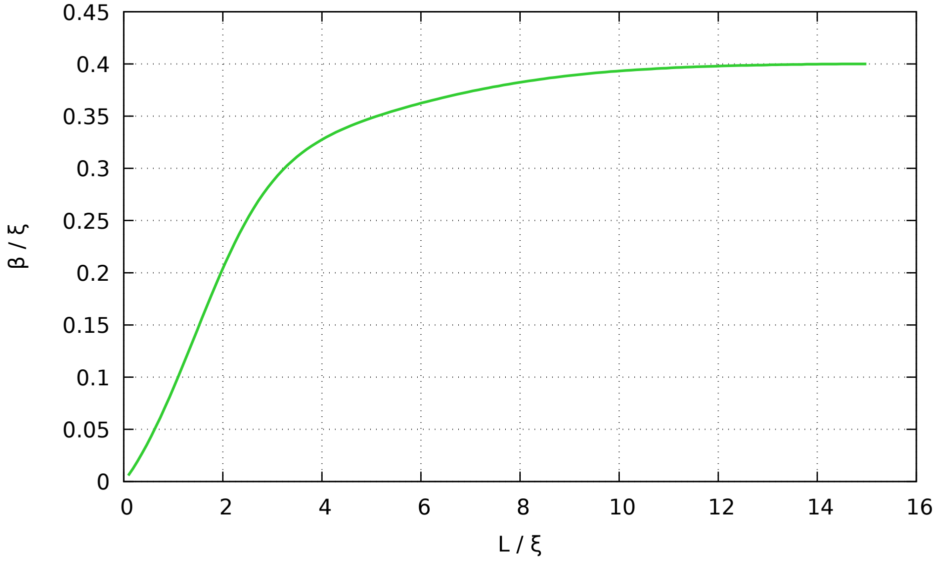

Figure 2.5: scaled β-vs-L at a distance $L/8$ away from the centre of the trap, at $z = 3L/8$.

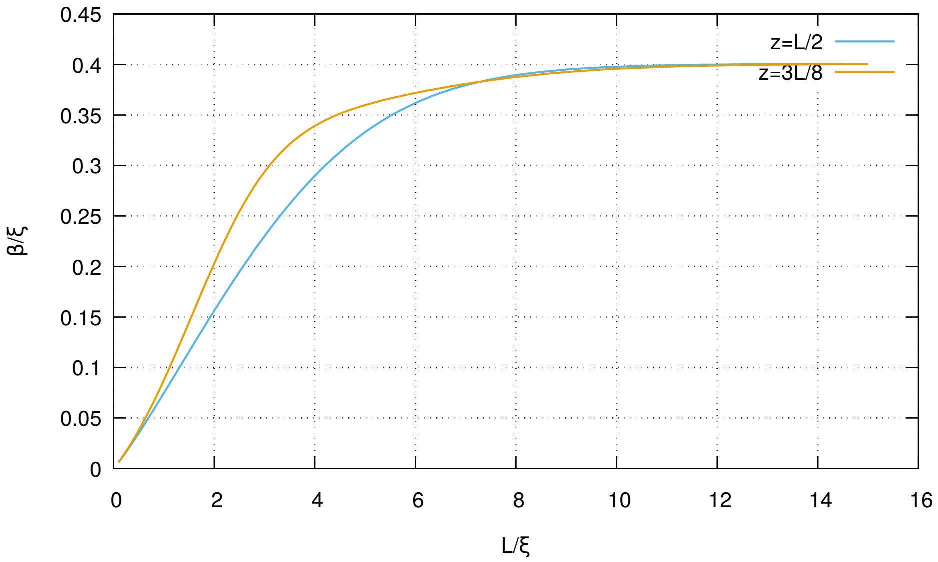

Figure 2.6: comparison of β-vs-L curve at $z = L/2$ and $z = 3L/8$.

Next thing to consider is how this trend changes as we move away from the center of the trap. This will give us a better idea of the profile of vortex width along z. After doing the same analysis for $z = 3L/8$, the graph that was obtained is shown in Fig.(2.5). We see that the trend is similar as that in the middle of the trap. The comparison of the trend at $z = L/2$ and at $z = 3L/8$ can be seen in Fig.(2.6). In the linear region, β for z value slightly away from the trap center is more than that in the middle. That means vortex expands as we move away from the center.

There are still a few points which need a closer look:

1) Closer to the boundaries of confinement, the observed trend disappears. This most probably is a consequence of unrealistic boundary conditions and neglecting $\partial\beta/\partial z$ term while deriving equations for $\tilde{h}(z)$ and $\beta(z)$. At the boundaries, faster variation of $\beta(z)$ is expected thus making this assumption invalid and leading to the break down of the solution. A more rigorous analysis with inclusion of $\partial\beta/\partial z$ terms is needed to understand the behaviour of vortex width along the whole range of z values.

2) The ansatz that we have considered gives a very complicated equation for β dynamics and makes it difficult to analyse the dependence of $\tilde{h}(z)$ profile on $\beta(z)$. A simpler ansatz is needed for a more tractable analysis. One such candidate would be $f(r, z) = 1 - e^{-r/\beta(z)}$.

It is easy to see that this ansatz satisfies the boundary conditions and will also be easier to work with due to the exponential factor.

3) Taking a closer look at the equations for C_2(2.9) and C_3(2.10), it can be seen that when β is a function of z, m and μ will also be functions of z. Having a gradient of chemical potential in the system means that there is a material flow to neutralise this current. This will make the state non-stationary unless the flow paths are in closed contours. This is a highly nontrivial condition and certainly requires a more involved analysis for the entire form of μ along z.

Summary: A semi-variational approach has been employed to understand the effect of z-confinement on vortex width. An ansatz is considered in r-direction to obtain the equation for z-profile, which is then solved exactly. Taking into account the variation of vortex width along z gives an expected result in large L limit. Also, for $L \sim \xi$, the vortex width is scaled by L and not ξ (at least near the center of the trap). Although this approach needs more refinement, it provides a possibility of producing thinner vortices by modulating confinement length in z.

Chapter 3

Axially-symmetric harmonic trap

In the previous chapter, we considered the effect of z-confinement on the core width of a vortex in BEC. In this chapter, we would bring in an additional length scale through confinement in r-direction and study how these two length scales (apart from the microscopic length scale in the system i.e. healing length) affect the vortex width.

Most common kind of trap is a harmonic trap, where potential goes as r^2. BEC under such harmonic trap has been well studied in strong interaction regime where the kinetic energy is negligible (Thomas-Fermi approximation), and the profile of the condensate is mostly dictated by interaction energy, excluding the boundary corrections [24]. Since interaction energy goes as n^2, its effect is seen as flattening of the condensate to avoid any density peaks. In this regime, the ground state profile is almost flat up to a certain radius R. Thus, we expect a vortex formed in this regime to have core width of the order of healing length. And so is the case as shown in ([24],[28]). Here, we want to study the other limit, *i.e.*, the weak interaction regime.

3.1 Variational approach

3.1.1 Taking appropriate ansatz

To get an effective dynamical equation in r-direction, the 3D GPE needs to be reduced to a quasi 2D equation. In the presence of axially symmetric trap, the GPE for vortex is:

$$\left[\frac{-\hbar^2}{2m}\left(\frac{1}{r}\frac{\partial}{\partial r}(r\frac{\partial}{\partial r}) - \frac{s^2}{r^2} + \frac{\partial^2}{\partial z^2}\right) + \frac{1}{2}m(\omega_r^2 r^2 + \omega_z^2 z^2) + g\Psi(r,z)^2\right]\Psi(r,z) = \mu\Psi(r,z) \quad (3.1)$$

$\Psi(r,z)$ is a real function and s is the angular momentum quantum number. Also, $\Psi(r,z)$ is normalised to the number of particles, N, in the condensate,

$$\int_{r=0}^{\infty}\int_{z\to-\infty}^{\infty} \mid \Psi(r,z) \mid^2 2\pi r^2 dr dz = N$$

This is one of the important differences between the current system and the system considered in the last chapter. In the previous system, due to an infinite extent in r, the far field density n could be fixed, while here, due to confinement, the number of atoms N has to be conserved.

Scaling the variables as $\tilde{z} = z/\sigma_z$, $\tilde{r} = r/\sigma_r$, where $\sigma_r = \sqrt{\hbar/m\omega_r}$ and $\sigma_z = \sqrt{\hbar/m\omega_z}$ are the oscillator lengths and $\Psi(r,z) = \sqrt{N/\sigma_r^2\sigma_z}\psi(\tilde{r},\tilde{z})$ such that

$$\int \mid \psi(\tilde{r},\tilde{z}) \mid^2 2\pi\tilde{r}^2 d\tilde{r} d\tilde{z} = 1 \quad (3.2)$$

the GPE in dimensionless form is obtained as,

$$\left[-\left(\frac{1}{\tilde{r}}\frac{\partial}{\partial\tilde{r}}(\tilde{r}\frac{\partial}{\partial\tilde{r}}) - \frac{s^2}{\tilde{r}^2} + \lambda\frac{\partial^2}{\partial\tilde{z}^2}\right) + (\tilde{r}^2 + \lambda\tilde{z}^2) + \frac{2gN}{\hbar\omega_r\sigma_r^2\sigma_z}\psi(\tilde{r},\tilde{z})^2\right]\psi(\tilde{r},\tilde{z}) = 2\tilde{\mu}\psi(\tilde{r},\tilde{z}) \quad (3.3)$$

where $\lambda = \omega_z/\omega_r$ and $\tilde{\mu} = \mu/\hbar\omega_r$. Putting $g = 4\pi\hbar^2 a_s/m$, we get,

$$\left[-\left(\frac{1}{\tilde{r}}\frac{\partial}{\partial\tilde{r}}(\tilde{r}\frac{\partial}{\partial\tilde{r}}) - \frac{s^2}{\tilde{r}^2} + \lambda\frac{\partial^2}{\partial\tilde{z}^2}\right) + (\tilde{r}^2 + \lambda\tilde{z}^2) + 8\pi\frac{Na_s}{\sigma_z}\psi(\tilde{r},\tilde{z})^2\right]\psi(\tilde{r},\tilde{z}) = 2\tilde{\mu}\psi(\tilde{r},\tilde{z}) \quad (3.4)$$

As we can see, the strength of the nonlinear term signifies the strength of interaction in the condensate and thus $8\pi\frac{Na_s}{\sigma_z}\psi(\tilde{r},\tilde{z})^2 >> 1$ is the TF regime while $8\pi\frac{Na_s}{\sigma_z}\psi(\tilde{r},\tilde{z})^2 < 1$ is the weak interaction regime.

In the following analysis, we are interested in a weakly interacting system. Also, the trap is taken such that the confinement in z is much tighter as compared to that in r which implies $\lambda >> 1$. In that case, $8\pi \frac{Na_s}{\sigma_z}\psi(\tilde{r},\tilde{z})^2 << \lambda$. Consider terms in Eq.(3.4) which determine the profile of condensate along z: $\lambda\frac{\partial^2\psi}{\partial z^2}$, $\lambda\tilde{z}^2\psi$ and $8\pi\frac{Na_s}{\sigma_z}\psi^3$. When $\lambda >> 8\pi\frac{Na_s}{\sigma_z}\psi(\tilde{r},\tilde{z})^2$, the contribution of the nonlinear term can be neglected while solving for the dynamics in z. Writing the wavefunction in a separable form as $\psi(\tilde{r},\tilde{z}) = f(\tilde{z})h(\tilde{z})$, the equation can then be easily decoupled to get $h(\tilde{z})$ dynamics as,

$$\left[-\frac{\partial^2}{\partial\tilde{z}^2} + \tilde{z}^2\right] h(\tilde{z}) = Kh(\tilde{z}) \tag{3.5}$$

K is a constant. Solving above equation, we get,

$$h(\tilde{z}) = e^{-\tilde{z}^2/2} \tag{3.6}$$

In the absence of interaction term, the dynamical equation in r would be,

$$\left[-\left(\frac{1}{\tilde{r}}\frac{\partial}{\partial\tilde{r}}(\tilde{r}\frac{\partial}{\partial\tilde{r}}) - \frac{s^2}{\tilde{r}^2}\right) + \tilde{r}^2\right] f(\tilde{r}) = (2\tilde{\mu} - \lambda)f(\tilde{r}) \tag{3.7}$$

This is the time independent Schrödinger equation with axially symmetric harmonic potential with $(2\tilde{\mu}-\lambda)$ as the eigenvalue. The stationary states of this equation are angular momentum eigenstates given as,

$$\left(\frac{r}{\sigma_r}\right)^s e^{-r^2/2\sigma_r^2} \tag{3.8}$$

s is the angular momentum quantum number. In the presence of the interaction term, we expect the spread of the wavefunction along r to change. Thus, combining (3.2, 3.6 and 3.8), following normalised trial wave function is considered for variational approach:

$$\Psi(r,z) = \sqrt{\frac{N}{\pi^{3/2}s!\sigma_z\beta^2}}\left(\frac{r}{\beta}\right)^s e^{-r^2/2\beta^2}e^{-z^2/2\sigma_z^2} \tag{3.9}$$

where β (that is, the width of the Gaussian in r), is now a variational parameter. Notice that width in z is still taken as σ_z since the nonlinear term does not significantly affect z-profile when $\lambda >> 1$, as discussed before.

3.1.2 Energy minimization

For a normalised wavefunction, we can consider energy instead of grand potential. The energy of the system can be written as

$$E = \int_r \int_z 2\pi r dr dz \left[\frac{\hbar^2}{2m} \left\{ |\frac{\partial \Psi}{\partial r}|^2 + \frac{s^2}{r^2}|\Psi|^2 + |\frac{\partial \Psi}{\partial z}|^2 \right\} + \frac{1}{2} m \left(\omega_r^2 r^2 + \omega_z^2 z^2 \right) |\Psi|^2 + \frac{g}{2} |\Psi(\mathbf{r})|^4 \right] \tag{3.10}$$

Putting the trial wavefunction (3.9) in this energy functional, we evaluate energy of the system as a function of β,

$$\begin{aligned} E(\beta) = \frac{2N}{s!} \left[\frac{1}{\beta^2} \left(\frac{\hbar^2}{2m} \frac{\Gamma(1+s)}{2} + \frac{\hbar^2}{2m} \frac{s^2 \Gamma(s)}{2} + \frac{2^{-(3+2s)} gN}{\pi^{3/2} s! \sigma_z} \frac{\Gamma(2s+1)}{\sqrt{2}} \right) \right] \\ + \frac{2N}{s!} \left[\beta^2 \left(\frac{m\omega_r^2}{2} \frac{\Gamma(s+2)}{2} \right) + E'(\sigma_z) \right] \end{aligned} \tag{3.11}$$

The term $E'(\sigma_z)$ does not depend on β and is merely the energy shift due to z-profile given as

$$E'(\sigma_z) = \frac{\hbar^2}{2m} \frac{\Gamma(1+s)}{4\sigma_z^2} + \frac{m\omega_z^2}{2} \frac{\Gamma(1+s)\sigma_z^2}{4}$$

In the expression(3.11), β^2 term is monotonically increasing while $1/\beta^2$ term is monotonically decreasing as a function of β and thus an energy minima is guaranteed given the coefficients of these two terms are positive. Let us take $s = 1$ for simplicity. To find β corresponding to minimum energy, we set $\partial E / \partial \beta = 0$. This gives

$$\beta^4 = \frac{1}{m\omega_r^2} \left[\frac{\hbar^2}{m} + \frac{gN}{8\sqrt{2}\pi^{3/2}\sigma_z} \right] \tag{3.12}$$

Putting $g = \frac{4\pi\hbar^2 a_s}{m}$ and $\frac{\hbar^2}{m^2\omega_r^2} = \sigma_r^4$, we get

$$\beta = \sigma_r \left[1 + \frac{1}{\sqrt{8\pi}} \frac{N a_s}{\sigma_z} \right]^{1/4} \tag{3.13}$$

It can be easily shown that maxima of the function Ψ as given in Eq.(3.9) is at $z = 0$ and $r = \beta$. Defining width of the vortex as full width at half maxima, the core width clearly scales as β. This together with Eq.(3.13) shows that in the weak interaction regime, vortex width (V_w) goes as

$$V_w \sim \beta = \sigma_r \left[1 + \frac{1}{\sqrt{8\pi}} \frac{N a_s}{\sigma_z}\right]^{1/4} \tag{3.14}$$

Let us analyse above expression (3.14).

1) β varies linearly with σ_r. The confinement length in r directly gets selected as vortex width. The healing length in such a confined system is defined as $\xi = 1/\sqrt{8\pi a_s n(0)}$ [29]. After performing a similar variational calculation for a non-vortex state to find $n(0)$, it can be shown that

$$\frac{\xi^2}{\beta^2} \sim \sqrt{\frac{\pi}{8}} \frac{\sigma_z}{a_s N} \tag{3.15}$$

Generally, the factor $a_s N/\sigma_z$ is taken to be small for weakly interacting system, thus giving $\xi > \beta$.

2) The effect of z confinement can be seen from the presence of σ_z in the correction term $\frac{1}{\sqrt{8\pi}} \frac{N a_s}{\sigma_z}$.

3) This correction term can also be tuned by changing the scattering length a_s using Feshbach resonance technique [30]. For a repulsive BEC, $a_s > 0$ resulting in the vortex width as well as the spread of the Gaussian to increase from σ_r. This is expected since repulsive interaction enegy, which goes as n^2, tries to reduce the density peak by pushing the condensate outwards. But a more interesting case is when $a_s < 0$ *i.e* attractive BEC.

Attractive BEC: An unbounded BEC with attractive interactions is unstable and collapses into a solid phase [32]. But in the presence of confinement, as the condensate peaks in the middle, the uncetaintly in momentum increases causing a kinetic pressure. It has been shown theoretically and experimentally that an attractive BEC can be stabilised inside a confinement ([33],[3]) till some maximum value of the interaction parameter $|\frac{N_c a_s}{\sigma_z}| \sim 0.57$ ([33],[34]). But experimentally, attractive condensates were found to be stable even beyond this maximum limit. This could be explained by the presence of a vortex line in the system [35]. Intuitively, this makes sense since the centrigular force due to rotation in the vortex opposes the inward pull due to attractive interactions. Thus, an attractive BEC system can be further stabilised by the presence of a vortex. Since attractive BEC is stable only in weak interaction regime, our approach is still valid.

When $a_s < 0$, the correction term in (3.14) becomes negative and thus reduces the vortex width from σ_r. By making the value of this correction term as close to -1 as possible, very

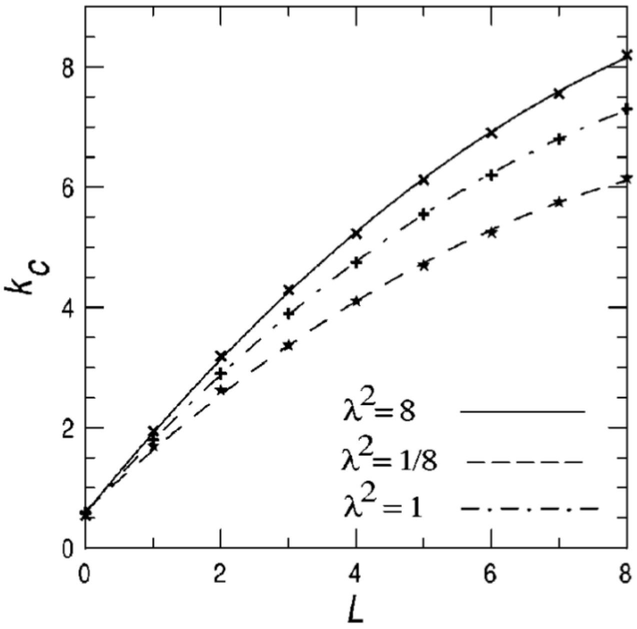

Figure 3.1: Critical value of $k_c = |\frac{Na_s}{\sigma_z}|$ vs L (angular momentum quantum number) for different ratios of $\frac{\omega_z}{\omega_r}$ (= λ in the plot). The figure is taken from [31].

thin vortices can be achieved. In the numerical calculation by S. Adhikari [31], the critical value of parameter $|\frac{Na_s}{\sigma_z}|$ has been evaluated for an axisymmetric trap like the one considered here. As seen in fig.(3.1), the critical value increases with increasing ratio ω_z/ω_r and with increasing vorticity. For a singly quantised vortex, the critical value can increase as much as 2.

When β reduces significantly in the case of $a_s < 0$, the change in the spread of the wavefunction in z direction might be significant. This has to be taken into account to see the lower limit for β.

3.2 Changed ansatz: attractive BEC

Let us consider the changed widths in r and z direction be D_r and D_z respectively. Thus the ansatz is

$$\Psi(r,z) = \sqrt{\frac{N}{\pi^{3/2} s! D_z D_r^2}} \left(\frac{r}{D_r}\right)^s e^{-r^2/2D_r^2} e^{-z^2/2D_z^2} \tag{3.16}$$

where now both D_r and D_z are variational parameters. The energy expression is

$$\begin{aligned} E(D_r, D_z) = \frac{2N}{s!}\left[\frac{1}{D_r^2}\left(\frac{\hbar^2}{2m}\frac{\Gamma(1+s)}{2} + \frac{\hbar^2}{2m}\frac{s^2\Gamma(s)}{2} + \frac{2^{-(3+2s)}gN}{\pi^{3/2}s!D_z}\frac{\Gamma(2s+1)}{\sqrt{2}}\right)\right] \\ +\frac{2N}{s!}\left[D_r^2\left(\frac{m\omega_r^2}{2}\frac{\Gamma(s+2)}{2}\right) + \frac{\hbar^2}{2m}\frac{\Gamma(1+s)}{4D_z^2} + \frac{m\omega_z^2}{2}\frac{\Gamma(1+s)D_z^2}{4}\right] \end{aligned} \tag{3.17}$$

The simultaneous minimization of energy with respect to both D_r and D_z will give coupled equations for them. Evaluating $\frac{\partial E}{\partial D_r} = 0$ gives

$$D_r = \sigma_r\left[1 + \frac{1}{\sqrt{8\pi}}\frac{Na_s}{D_z}\right]^{1/4} \tag{3.18}$$

just as Eq.(3.14) but with σ_z replaced by D_z. Also, $\frac{\partial E}{\partial D_z} = 0$ gives

$$\left(\frac{D_z}{\sigma_z}\right)^4 - \frac{Na_s}{\sqrt{2\pi}\sigma_z}\frac{\sigma_z^2}{D_r^2}\left(\frac{D_z}{\sigma_z}\right) - 1 = 0 \tag{3.19}$$

When the second term in the above equation $\frac{Na_s}{\sqrt{2\pi}\sigma_z}\frac{\sigma_z^2}{D_r^2}$ is small, the expression for D_z can be given as

$$D_z \sim \sigma_z\left(1 + \frac{Na_s}{4\sqrt{2\pi}\sigma_z}\frac{\sigma_z^2}{D_r^2}\right) \tag{3.20}$$

Notice that when the interaction parameter $\frac{Na_s}{\sigma_z}$ is small, the correction to $D_r \sim \frac{1}{4\sqrt{8\pi}}\frac{Na_s}{D_z}$ is much greater than the correction to $D_z \sim \frac{Na_s}{\sqrt{2\pi}\sigma_z}\frac{\sigma_z^2}{D_r^2}$ when $\frac{\sigma_z^2}{D_r^2} << 1$. This is true when the confinement is considered to be much tighter in z than in r (that is $\lambda >> 1$). In this case, $D_z \sim \sigma_z$ in the expression for D_r (3.18). As expected, this yeilds the same result as that derived in the previous section.

As D_r reduces to very small values due to negative a_s, the second term in (3.20) is no longer small and the deviation in D_z from σ_z can no longer be neglected. This also shows that D_r can not be made arbitrarily small since this second term will diverge and thus there should be some kind of minimum value for D_r before the vortex solution breaks down.

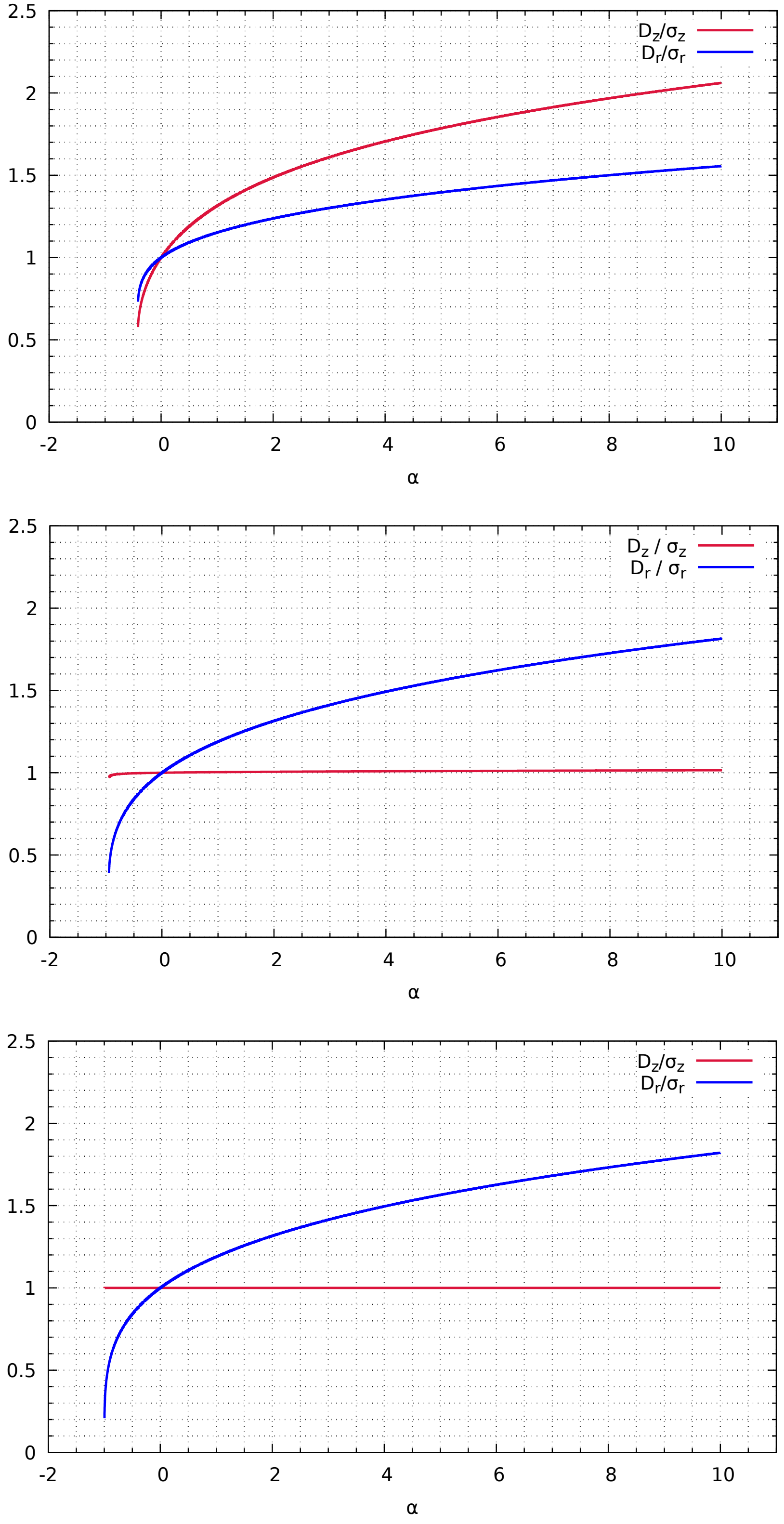

Figure 3.2: Variation of D_r and D_z with $\alpha = \frac{Na_s}{\sqrt{8\pi}\sigma_z}$ for different values of ratio $\frac{\sigma_r}{\sigma_z}$: (a)$\frac{\sigma_r}{\sigma_z} = 1$, (b) $\frac{\sigma_r}{\sigma_z} = 10$, (c) $\frac{\sigma_r}{\sigma_z}$ =100

Fig.(3.2)(b) shows the curve of $\frac{D_r}{\sigma_r}$ and $\frac{D_z}{\sigma_z}$ as a function of parameter $\alpha = \frac{Na_s}{\sqrt{8\pi}\sigma_z}$ for a fixed value of $\frac{\sigma_r}{\sigma_z} = 10$. Here are some important points to notice:

1) As a_s decreases from positive to negative values, the width of the wavefunction in r decreases non-linearly till some minimum value of a_s is reached. This agrees with the expectation.

2) The $\frac{D_z}{\sigma_z}$ varies much slower than $\frac{D_r}{\sigma_r}$ curve as expected.

3) The curves have tilted parabolas-like shape. The lower halves of these curves correspond to an energy maxima.

4) Through graphs (a) to (c), it can be seen that the lowest value of α, which still gives the vortex solution, decreases with increasing ratio of $\frac{\sigma_r}{\sigma_z}$. By making the confinement in z-direction tighter as compared to that in r, smaller values to a_s can be reached, which will also make the vortex thinner. In Fig.(3.2)(c), for $\frac{\sigma_r}{\sigma_z} = 100$, D_r can be made as small as $0.2\sigma_r$.

5) As expected, the variation in D_z from σ_z becomes neglible as the ratio $\frac{\sigma_r}{\sigma_z}$ becomes large.

Summary: The length scale of vortex width changes from ξ to the characteristic length of the trap σ_r in weak interaction limit. The width can be further reduced by making the interactions attractive. This can be done by changing the scattering length to negative values using Feshbach resonance. The maximum negative value of a_s which still gives an energy minima increases by increasing the ratio σ_r/σ_z. In effect, a thinner vortex can be achieved by increasing σ_r/σ_z and making a_s as small as possible, while still remaining in the weak interaction regime.

Chapter 4

Conclusion and future work

It is possible to modulate the vortex core width by changing the confinement length in certain parameter regimes. For a large system with fixed far field density, confined in z by hard boundaries, the vortex width near the centre varies as the length of confinement (L) when this length is of the order of healing length. In another system, with axisymmetric harmonic trap, the vortex width can be significantly reduced by making the interactions attractive. Both the systems are quite promising in achieving the aim of small filling fractions by making the vortices thinner.

In future, above analytical results can be verified by numerical simulations. Once verified, the analysis can be extended to a vortex lattice rather than a single vortex. This will include vortex-vortex interaction effects and will be closer to the experimental situation. Also, the stability of these structures can be analysed by studying the excitation spectrum.

Bibliography

[1] Mike H Anderson, Jason R Ensher, Michael R Matthews, Carl E Wieman, and Eric A Cornell. Observation of Bose-Einstein condensation in a dilute atomic vapor. *science*, 269(5221):198, 1995.

[2] K. B. Davis, M. O. Mewes, M. R. Andrews, N. J. Van Druten, D. S. Durfee, D. M. Kurn, and W. Ketterle. Bose-Einstein condensation in a gas of sodium atoms. *Physical Review Letters*, 75(22):3969–3973, 1995.

[3] C. C. Bradley, C. A. Sackett, J. J. Tollett, and R. G. Hulet. Evidence of Bose-Einstein condensation in an atomic gas with attractive interactions. *Physical Review Letters*, 75(9):1687–1690, 1995.

[4] Alexander L. Fetter. Rotating trapped Bose-Einstein condensates. *Reviews of Modern Physics*, 81(2):647–691, 2009.

[5] C. J. Pethick and H. Smith. *Bose-Einstein Condensationin Dilute Gases*. Number 1991. 2008.

[6] Y Castin and R Dum. Bose-Einstein condensates with vortices in rotating traps. *J. of Phys. D*, 412:399, 1999.

[7] D a Butts and D S Rokhsar. Predicted signatures of rotating Bose-Einstein condensates. *Nature*, 397(1998):327–329, 1999.

[8] J R Abo-Shaeer, C Raman, J M Vogels, and W Ketterle. Observation of Vortex Lattices in Bose-Einstein Condensates. *Science*, 292(5516):476–479, 2001.

[9] Academisch Proefschrift and J. W. Reijnders. Quantum Phases for rotating bosons door. 2005.

[10] Uwe R Fischer and Gordon Baym. Vortex states of rapidly rotating dilute Bose-Einstein condensates. *Physical review letters*, 90(14):140402, 2003.

[11] Gordon Baym and C J Pethick. Vortex core structure and global properties of rapidly rotating Bose-Einstein condensates. *Physical Review A*, 69(4):43619, 2004.

[12] I Coddington, P C Haljan, Peter Engels, Volker Schweikhard, Shihkuang Tung, and Eric A Cornell. Experimental studies of equilibrium vortex properties in a Bose-condensed gas. *Physical Review A*, 70(6):63607, 2004.

[13] T L Ho. Bose-Einstein condensates with large number of vortices. *Physical review letters*, 87(6):060403, 2001.

[14] Volker Schweikhard, I Coddington, Peter Engels, V P Mogendorff, and Eric A Cornell. Rapidly rotating Bose-Einstein condensates in and near the lowest Landau level. *Physical review letters*, 92(4):40404, 2004.

[15] Jairo Sinova, Charles B Hanna, and A H MacDonald. Quantum melting and absence of Bose-Einstein condensation in two-dimensional vortex matter. *Physical review letters*, 89(3):30403, 2002.

[16] Nigel R Cooper, Nicola K Wilkin, and J M F Gunn. Quantum phases of vortices in rotating Bose-Einstein condensates. *Physical review letters*, 87(12):120405, 2001.

[17] N K Wilkin and J M F Gunn. Condensation of composite bosons in a rotating BEC. *Physical review letters*, 84(1):6, 2000.

[18] Nicolas Regnault and Th Jolicoeur. Quantum Hall fractions in rotating Bose-Einstein condensates. *Physical review letters*, 91(3):30402, 2003.

[19] Nicholas Read and E Rezayi. Beyond paired quantum Hall states: parafermions and incompressible states in the first excited Landau level. *Physical Review B*, 59(12):8084, 1999.

[20] N R Cooper and N K Wilkin. Composite fermion description of rotating Bose-Einstein condensates. *Physical Review B*, 60(24):R16279, 1999.

[21] Vincent Bretin, Sabine Stock, Yannick Seurin, and Jean Dalibard. Fast rotation of a Bose-Einstein condensate. *Physical review letters*, 92(5):50403, 2004.

[22] Anders S S\orensen, Eugene Demler, and Mikhail D Lukin. Fractional Quantum Hall States of Atoms in Optical Lattices. *Phys. Rev. Lett.*, 94(8):86803, mar 2005.

[23] Y-J Lin, Rob L Compton, K Jimenez-Garcia, James V Porto, and Ian B Spielman. Synthetic magnetic fields for ultracold neutral atoms. *Nature*, 462(7273):628–632, 2009.

[24] Lev Pitaevskii and Sandro Stringari. *Bose-Einstein condensation and superfluidity*, volume 164. Oxford University Press, 2016.

[25] Jerome Spanier. *An Atlas of Functions*, volume 56. 1988.

[26] L. D. Carr, Charles W. Clark, and W. P. Reinhardt. Stationary solutions of the one-dimensional nonlinear Schrodinger equation. I. Case of repulsive nonlinearity. *Physical Review A - Atomic, Molecular, and Optical Physics*, 62(6):063610–063611, 2000.

[27] L. Salasnich, A. Parola, L. Reatto, and a. Parola. Effective wave equations for the dynamics of cigar-shaped and disk-shaped Bose condensates. *Phys. Rev. A*, 65(4):43614, 2002.

[28] Z Nikolas. A Single Vortex in a Bose-Einstein Condensate Bachelor Thesis by. 2010.

[29] Alexander L Fetter and Anatoly A Svidzinsky. Vortices in a trapped dilute Bose-Einstein condensate. *Journal of Physics: Condensed Matter*, 13(12):R135–R194, 2001.

[30] S Inouye, M R Andrews, J Stenger, H-J Miesner, D M Stamper-Kurn, and W Ketterle. Observation of Feshbach resonances in a Bose–Einstein condensate. *Nature*, 392(6672):151–154, 1998.

[31] Sadhan K Adhikari. Collapse of attractive Bose-Einstein condensed vortex states in a cylindrical trap. 65:1–9, 2001.

[32] H T C Stoof. Atomic Bose-Gas With a Negative Scattering Length. *Physical Review A*, 49(5):3824–3830, 1994.

[33] P. A. Ruprecht, M. J. Holland, K. Burnett, and Mark Edwards. Time-dependent solution of the nonlinear Schrödinger equation for Bose-condensed trapped neutral atoms. *Physical Review A*, 51(6):4704–4711, 1995.

[34] C C Bradley, C A Sackett, and R G Hulet. Bose-Einstein condensation of lithium: Observation of limited condensate number. *Physical Review Letters*, 78(6):985, 1997.

[35] F Dalfovo and S Stringari. Bosons in anisotropic traps: Ground state and vortices. 53(4), 1996.